**Project Title:**

# Nucleon Structure from Lattice QCD with Domain Wall Fermions

Name:○Meifeng Lin(5)(1), Tom Blum(2)(1), Taku Izubuchi(4)(1), Chulwoo Jung(4)(1),
    Shigemi Ohta(6)(7)(1),  Shoichi Sasaki(8)(1),  Takeshi Yamazaki(9)(1)

Laboratory:
(1) Theory Group, RIKEN BNL Research Center, Sub Nuclear System Research Division, RIKEN Nishina Center for Accelerator-Based Science, RIKEN Wako Institute
(2) Department of Physics, University of Connecticut
(3) Department of Physics, University of Virginia
(4) Physics Department, Brookhaven National Laboratory
(5) Center for Computational Science, Boston University
(6) Institute of Particle and Nuclear Studies, KEK
(7) Department of Particle and Nuclear Physics, Sokendai Graduate University of Advanced Studies
(8) Department of Physics, Tohoku University
(9) Center for Theoretical Studies, Nagoya University

## Description of the project

### 1. Introduction

#### 1.1 Scientific Background

Protons and neutrons (collectively called nucleons) compose the major part of atoms, and are fundamental building blocks of the visible matter. Understanding their internal structure advances our fundamental knowledge about the composition of the universe, and is a top-priority topic of the US Department of Energy (DOE) nuclear physics long-range plan. Many particle and nuclear experiments worldwide are actively probing the charge, current, magnetization and other fundamental properties of protons and neutrons, such as Mainz in Germany and the Jefferson Lab in the US. In particular, the RIKEN-sponsored RHIC-Spin experiment at Brookhaven National Laboratory in the US probes the spin structure of the nucleon, and one of the main motivations of our project is to be able to compare the theoretical predictions from lattice QCD calculations with the RHIC experiments. From a theorist's point of view, being able to interpret the observed experimental data and predict new properties of the nucleons from first-principles theories enhances our fundamental understanding of the underlying interactions and is the ultimate goal of our proposed research topic.

The theory that describes the interactions inside a proton is the so-called Standard Model of particle physics. In particular, we are interested in the component of the Standard Model known as Quantum Chromodynamics (QCD). In this theory, a proton consists of quarks which are fermions with fractional charges, and gluons which mediate the strong interactions among quarks. Because of the nature of the strong interactions, traditional perturbative theoretical calculations (which assume that fermions receive only small corrections to their behavior from the force carrying bosons) fail to work. In the 1970s Kenneth Wilson (later to win the Nobel Prize for his work on the Renormalization Group and Critical Phenomena) formulated Lattice QCD. This did two things: firstly, it provided a rigorous definition of the meaning of QCD beyond perturbation theory, and secondly it provided a way to perform first-principles calculations numerically. While it has taken several decades of improvements in computing power and algorithmic developments, recently the latter has been very successful in reproducing observed experimental data, such as the particle spectrum and decay properties. In lattice

QCD calculations, the four-dimensional space-time is discretized into a box with discrete grid points, and Monte Carlo simulations based on the Standard Model are carried out on computers. Since lattice QCD simulations are carried out in a finite box, at finite quark masses and at a finite lattice spacing, before we can reliably interpret our results, we need to have the associated systematic errors under control.

The two most prominent systematic errors may be the errors associate with the finite volume and finite quark masses in the lattice calculations. In order to relate the results from lattice simulations to the real world, extrapolations are required to obtain results at the physical point which can then be compared to known experimental values or as predictions for future experiments. Chiral perturbation theory (ChPT), a low-energy effective theory, is often used to guide the extrapolation. However, at the order practical for our calculation, chiral perturbation theory is only applicable at small quark masses (or equivalently, small pion masses). Existing lattice calculations of nucleon structure with chiral fermions have pion masses only as low as 300 MeV (while the physical pion mass is about 140 MeV), which are at the edge of the applicability of chiral perturbation theory of the appropriate order [1,2,3,10]. It has been found that lattice results at these pion masses are not consistent with the predictions of chiral perturbation theory, and the extrapolated values using ChPT deviate from the experimental values, indicating the systematic errors from chiral extrapolations are large [3,4,6,10,12]. Doing lattice calculations at lighter pion masses will greatly reduce the uncertainty associated with the chiral extrapolation and has the potential of producing high-precision results valuable to both the theory and experiment communities.

As the pion mass gets lighter, the pion Compton wavelength gets larger, and the size of the lattice volume needs to be larger to accommodate the pions. On the other hand, as the pion mass gets lighter and the volume gets larger, the numerical cost of the lattice calculations increases dramatically. Due to the complexity, and expense, of such calculations, there are naturally large research collaborations to facilitate the research efforts.

The RIKEN-BNL-Columbia (RBC) collaboration started around the same time as the RIKEN-BNL Research Center (RBRC) was founded in 1997. RIKEN and Columbia jointly built the 600-GFlops QCDSP (Quantum Chromodynamics on Digital Signal Processors) computer dedicated for lattice-QCD numerical research at RBRC. The RBC also pioneered the use of a particular formulation of lattice QCD known as Domain Wall Fermions (DWF)[14]. Traditional lattice formulations break many of the symmetries of the continuum theory. Perhaps the most important of these is chiral symmetry which says that left-handed and right-handed quarks are only coupled due to the small mass terms of the quarks. Naive lattice QCD formulations lead to couplings which are orders of magnitude too large. In DWF an additional fifth dimension is introduced to the space-time, with the left- and right-handed fermions living on opposite four-dimensional boundaries of the five-dimensional space, which greatly improves chiral symmetry. This formulation revolutionized the way numerical lattice QCD research is conducted. An important outcome was that the so-called non-perturbative renormalization method became practical, and made possible, for the first time in history, accurate calculations of quantum transitions between hadronic states.

1.2 Purpose of the Project

The purpose of this multi-year project is to calculate the structure of nucleons using lattice QCD techniques. The primary focus of this research is to

calculate all the isovector vector- and axial-vector form factors and some low moments of isovector structure functions of nucleon using a new set of lattice QCD numerical ensembles at larger than ever spatial volume of about 4.5 fm across and pion masses as low as[1] 170 MeV [13, 21]. An exploratory study of the nucleon strangeness content will also be pursued. We also propose to use a small fraction of the time for algorithmic developments. Detailed descriptions of each topic are given below.

(1) Precision lattice determination of nucleon mass. Being able to reproduce the experimentally well-known nucleon mass from the first-principles lattice calculations is a first step in establishing the precision test of lattice QCD. Previously, the heavy pion masses in the calculations make it hard to perform chiral extrapolations. With nearly physical pion mass in our calculations, we will be able to obtain a nucleon mass which is free of large systematic errors coming from chiral extrapolations. We will also be able to investigate the validity of chiral perturbation theory in these small pion mass ranges. Such calculations will be a great milestone towards high-precision lattice calculations.

(2) Nucleon vector form factors. Nucleon isovector vector form factors are part of the electromagnetic form factors and thus studied mainly by elastic electromagnetic processes such as electron scattering off nucleons or nuclei. They provide information of such important properties as mean-squared charge radii or anomalous magnetic moments which determine electromagnetic interactions of nuclei with other electromagnetic entities such as photon and electron. Thus these form factors ultimately

determine electromagnetic properties of atoms which in turn govern properties of chemistry and biology.

Because the quark masses in lattice calculations are heavier than reality, extrapolations that utilize the formula given by chiral perturbation theory are needed. In order to be able to reliably apply the chiral formula, the quark masses in the simulations need to be small enough. Previous lattice calculations have pion masses usually larger than 300 MeV, while a physical pion mass is about 140 MeV, which requires a long extrapolation from the simulated data to the physical point. Performing lattice calculations on the new DWF ensembles at pion masses of 250 MeV and 170 MeV will significantly reduce the systematic errors coming from chiral extrapolations. In addition, the large volume of the new ensembles will make the calculations less susceptible to finite volume effects and have the potential of achieving unprecedented statistical and systematic precisions.
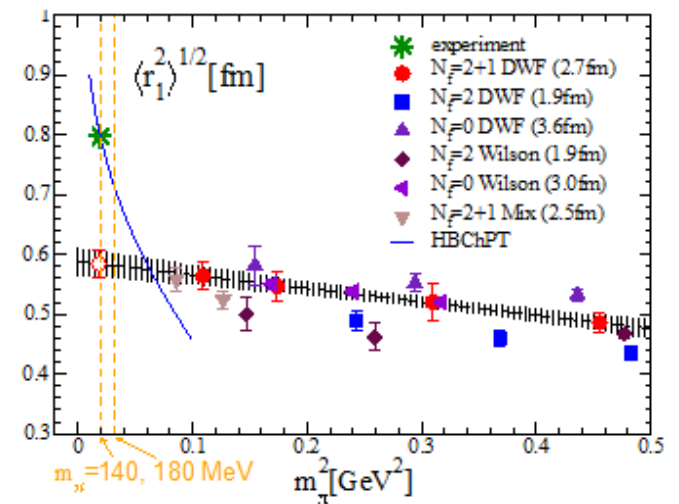


Figure 1: Nucleon isovector charge radii from previous lattice calculations. The green star is the experimental point, and the blue curve is prediction from chiral perturbation theory.

Given in Fig.1 are the results from previous lattice calculations for the nucleon isovector Dirac radii as a function of the pion mass squared, where the lattice results are systematically lower than the

---

[1] We note that the pion mass for the light ensemble was previously determined to be 180 MeV. New improved measurements gave a result of 170 MeV. Thus in this report, we refer this ensemble as 170 MeV ensemble.

experimental point and are not consistent with the prediction from chiral perturbation theory. A naive linear extrapolation to the lattice data gives a value at the physical point which is much smaller than expected. Having lattice results at lower pion masses will undoubtedly improve our ability to perform a more reliable chiral extrapolation.

(3) Nucleon axial form factors. Nucleon axial and induced pseudoscalar form factors probe the weak structure of the nucleon, and are also actively pursued experimentally, for example by using muon instead of electron: muon capture process is sensitive to a part of these form factors, $g_P$, for example.

The nucleon axial charge $g_A$ is defined as the zero momentum-transfer limit of the axial form factor, and determines the neutron lifetime. It is indeed best measured in neutron beta decay, in which a neutron decays into a proton via weak interaction and emits an electron and anti-neutrino. It also controls the interaction of pion and nucleon through the Goldberger-Treiman relation. Thus it is the single most important nucleon property in determining the abundance of elements that are formed in premordial and stellar nucleosynthesis. In contrast to the corresponding vector charge, $g_V$, which is not affected by the strong interaction, it receives corrections from the strong interaction and deviates from unity in units of $g_V$, $g_A = 1.2701(25) \, g_V$. We recently discovered this strong correction is strongly dependent on the pion mass and the volume in which the lattice calculation is conducted. This is shown in Fig. 2, where lattice results from different lattice volumes and different lattice formulations depend not only on the pion masses, but also the volumes. Our current calculations will continue to explore the dependence of $g_A$ on the pion mass and the lattice volume, and allow us to perform a more reliable extrapolation to obtain a physical value for $g_A$.
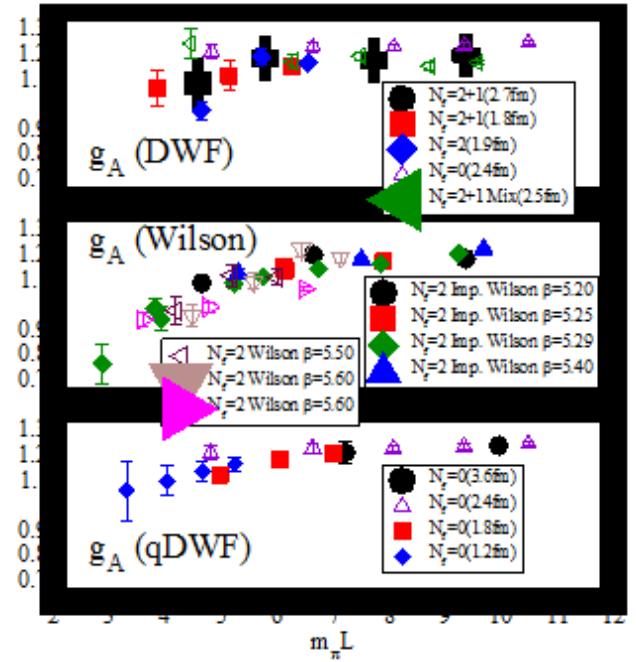


Figure 2: $m_\pi L$-scaling for $g_A$, which indicates finite volume effects.

(4) Nucleon structure functions. Studied mainly by lepton deep inelastic scattering and Drell-Yan experiments off nucleon and nuclei, these reveal deeper structures of nucleon and led to discovery of quarks and QCD. RIKEN experimenters are trying to resolve a puzzle in spin-dependent structure functions of nucleon through the RHIC-Spin experiments now conducted at RIKEN-BNL Research Center. Of particular interest are the quark momentum fraction, helicity fraction, and tensor charge, all in isovector combinations.

For the first two quantities conventional lattice-QCD numerical calculations significantly over estimate the experimental values. A recent joint study by RBC and UKQCD collaborations found that at the lightest quark mass value that corresponds to 330 MeV pion mass these values trend down to the experiment. By comparing the two different volumes, it is suggested the finite-size effects in these quantities seem absent, in contrast to the situation for the axial form factors discussed in the above. It is thus interesting to see if the trend toward experiment and apparent absence of the finite-size effect hold at the lighter quark

masses that correspond to 250 MeV and 170 MeV pions.

For tensor charge the same joint RBC/UKQCD study have a crude prediction. As this quantity will soon be experimentally measured, it is obviously important to refine this prediction at lighter quark mass values.

(5) Strangeness content of the nucleon. There has been much interest in a more accurate evaluation of scalar matrix elements of nucleons, in particular due to its connection to the coupling of nucleons to MSSM (Minimal Supersymmetric Standard Model) dark matter candidates via Higgs boson. However, lattice calculation of this quantity has been a challenge, due to the fact that the traditional method of calculating such quantities involves evaluation of what is known as disconnected diagrams, which are intrinsically noisy and so, when using standard techniques, require a large number of measurements. Recent studies with a formulation of lattice QCD known as Overlap fermions suggest the preservation of chiral symmetry is crucial in controlling systematic errors, suggesting a DWF calculation would be advantageous.

Recently there have been lattice studies using Feynman-Hellman theorem, which showed promise in calculating the scalar matrix element without expensive evaluation of disconnected diagrams, but rather via a calculation of the derivative of much less expensive observables with respect to the strange quark mass. Here we propose to evaluate the nucleon scalar matrix element by taking such a numerical derivative of the nucleon mass via what is known as a reweighting; a technique we have recently successfully applied to modifying the strange quark mass of our lattice gauge configurations [20].

(6) Algorithmic development. The choice of which problems to address using lattice techniques is constrained by the algorithms available to both generate the lattice gauge field configurations, and calculate quantities using them. While the increase in available computer power over the past few years has played a vital role in making Lattice QCD a realistic tool for studying QCD, algorithmic improvements have played a role at least as important, and we propose to use a small portion of the computer time covered by this proposal to continue such developments.

2. Computational Details and Usage Status

2.1 Computational Methods

We perform our calculations with domain wall fermions on the existing gauge backgrounds generated by the RBC and UKQCD collaborations. These gauge backgrounds encode a particular configuration of the gluon fields. For each such configuration we need to calculate the sum of all possible paths a quark can take between a given set of starting positions (sources) and all points on the lattice. While other calculations will be involved, this will be the dominant calculation in terms of computer time. The natural unit in which to measure such things is a single starting position. A single starting position leads to the calculation of a single quark propagator. To make the best use of the available gauge backgrounds, we plan to calculate quark propagators at four independent starting positions. From each propagator four so-called sequential propagators will be needed to perform the proposed calculations. The sequential propagators will then multiply the forward propagator from the source with appropriate operators and momentum of interest. Thus on each gauge background, 20 propagators are needed.

Once the forward propagators and the sequential propagators are calculated, we construct two and three-point functions of the nucleon. The two-point

nucleon correlation functions are traces of the products of the forward propagators, and the three-point functions are traces of the products of the forward propagators and sequential propagators. A graphical representation of the so-called connected diagram of the three-point function is shown in Fig.3.
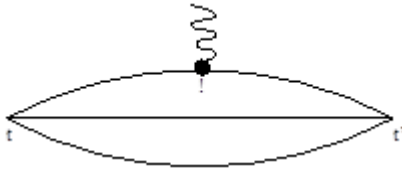


Figure 3: An illustration of the connected contribution to the nucleon three-point functions. t and t' are the locations of the nucleon source and sink, respectively. τ is the location of the operator of interest.

In addition to the connected contribution, another type of diagram also exists except in the isovector limit. This type of diagram is shown in Fig. 4, and is called the disconnected diagram. We are not considering this in most of our calculations, and only investigate it in our algorithmic development phase.
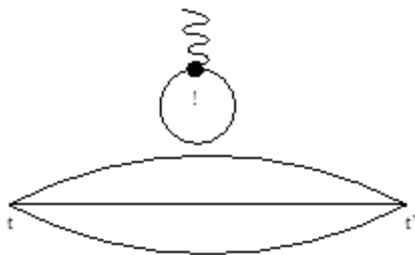


Figure 4: An illustration of the disconnected contribution to the nucleon three-point functions. t and t' are the locations of the nucleon source and sink, respectively. τ is the location of the operator of interest.

Since we perform Monte Carlo simulations, we will need to do the calculations on multiple gauge backgrounds so that statistical averages and errors can be calculated. We perform the calculations on the gauge backgrounds separated by 8 time units to reduce the autocorrelations between measurements.

Since we are interested in the properties of the nucleon ground state, we need to make sure that the operator insertion τ is within the asymptotic region where the nucleon ground state dominates. Hence we need to choose the source-sink separation $t' - t$ such that it is large enough to eliminate the excited state contaminations which are exponentially decaying with the distance from the source. However, as the source-sink separation $t' - t$ gets larger, gauge fluctuations generate more noise, which makes the already-difficult-to-get signal worse. Thus the first step is to choose an optimal source which has a good overlap with the nucleon ground state, so that we do not have to have a very large source-sink separation to be able to do nucleon ground state physics. This is the source-tuning process which is done before production runs begin.

We have determined from our calculations that a Gaussian smeared source with a width of 6 units is optimal for our study. And a source-sink separation of 9 lattice units in the time direction will be large enough to suppress excited-state contaminations while at the same time small enough to guarantee reasonable signals.

We have also implemented and tested an improved technique to calculate the sequential propagators. The technique is described below.

Because every physical observable has to be gauge invariant, any gauge-variant contractions will vanish over a large, statistically independent, gauge ensemble. This property leads to the so-called "coherent-sink trick" [3], in which sequential

propagators for different forward propagators can be computed simultaneously. If we have a three-point function constructed from a forward propagator and an independently calculated sequential propagator from that forward propagator, the contraction looks like Fig. 5(a). When multiple sequential propagators are calculated at the same time, in addition to the diagram in Fig. 5(a), we will also have diagrams like Fig. 5(b), where the red lines are contaminations from the other sources. Note that the blue line is in no way connected to the red lines, as they come from different sources. Hence this diagram is not gauge invariant, and should average to zero over a large gauge ensemble.
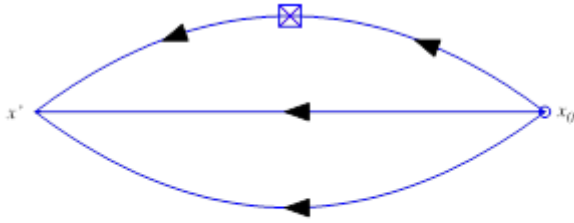


(a)The usual nucleon three-point contraction from a forward propagator and an independently calculated sequential propagator.
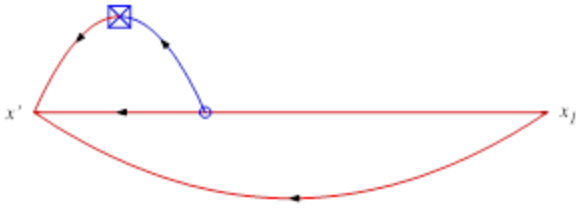


(b)The contamination from the other source to the nucleon three-point function with the *coherent-sink* method. The red lines are propagators from the other source(s).

Figure 5: Contributions to the nucleon three-point correlation functions.

This allows us to calculate the sequential propagators corresponding to different sources on one lattice simultaneously, instead of having to calculate sequential propagators for different sources separately. For our calculations with four sources per lattice, originally 16 sequential propagator calculations are needed (4 per source). With this new technique, we will also need to do 4 sequential propagator calculations, earning us a factor of 4 reduction in computation time compared to the original method.

While the calculations described in the previous section form the framework of our project, alone they are not sufficient to reduce the statistical error on computed, physical, quantities to the 5% level, or below, necessary to test the theory and experiment. To get to this level, especially for the 170 MeV pion mass ensemble, so-called all-mode averaging (AMA)[22] is needed. AMA requires the computation of the lowest eigenmodes of the Dirac operator and corresponding eigenvectors of the Dirac operator in order to construct the low-mode part of the quark propagator, $S_l$, and then the part of correlation function, $O_l$, is constructed from $S_l$. The high-mode part of the observable can be approximated with sloppy CG (conjugate gradient with a relaxed stopping condition of the order of 1e-3, instead of the typical 1e-8 in the conventional calculations). So the original observable $O$ is divided into the approximate part, $O_{appr}$ and the correction part, $O_{rest}$, so that $O = O_{appr} + O_{rest}$.

Since the statistical ensemble has the invariance under the translational invariance G due to the symmetry of the action used, and the construction of $O_{appr}$ is covariant under G, the following equation for the statistical average under the observable $\langle O \rangle$ holds: $\langle O_{appr} \rangle = \langle O_{appr}^G \rangle$, where $\langle O_{appr}^G \rangle$ is the observable under the symmetry transformation G. The ensemble average for the observable $\langle O \rangle$ can

now be determined as $\langle O \rangle = \langle O_{AMA} \rangle + \langle O_{rest} \rangle$, where

$O_{AMA} = \frac{1}{N_G} \sum_G O_{appr}^G$ is the all-mode-averaging part of the

observable $O$ averaged over $N_G$ symmetry transformations with sloppy CG. Since translation is a symmetry in our action, G can be taken to be just the shift of the lattice coordinates, allowing us to average the correlation functions over the entire four-volume of the lattice and increase the statistics significantly with negligible extra computing cost once the low eigenmodes have been calculated.

To correct for the bias in $\langle O_{AMA} \rangle$ due to sloppy CG, $\langle O_{rest} \rangle$ needs to be determined. We do this by performing (much fewer) exact calculations on the same gauge configuration, such that

$$O_{rest} = \frac{1}{N_{exact}} \sum O_{exact} - \frac{1}{N_G} \sum_G O_{appr}^G .$$

Note that $N_{exact}$ is typically of O(1), while $N_G$ is of O(100).

### 2.2 Usage Status

As of today (March 3, 2013), we have used 72% of our allocation of 3924992 core*hours. Our running on RICC was slowed from October to January, when we were implementing and testing the code to apply the AMA method described in Section 2.1. Due to the memory limitation of the RICC systems, we found that we were not able to calculate the low-mode part of the AMA, and opted to perform the exact parts of the calculations on RICC. The numbers of exact propagators we have calculated are listed in Table 1.

Table 1: The total numbers of propagators completed from April 1 2012 to March 3, 2013.

| Pion Mass | # f.p. | # s.p. | Total |
|-----------|--------|--------|-------|
| 170 MeV   | 151    | 386    | 537   |
| 250 MeV   | 108    | 428    | 536   |

### 3. Preliminary Results

The resources we have used on RICC allowed us to obtain substantial statistics to perform improved analysis of the key observables we outline in Section 1. In particular, we have obtained improved results for the nucleon axial charge, nucleon vector and axial vector form factors and the nucleon strangeness content. Even though a publication in refereed journals is still a work-in-progress, we have presented our preliminary results at several international conferences and symposiums [18,19]. We summarize some of our preliminary results below. Some of these results have been published in conference proceedings (see List of Publications).

### 3.1 Nucleon axial charge

As we mentioned previously, being able to calculate nucleon axial charge on the lattice serves as a precision test of QCD.

In Figure 7, we plot our results from the 170 MeV and 250 MeV ensembles (blue stars) along with recent RBC results (red crosses) as a function of $m_\pi L$. The 250 MeV result agrees with the earlier calculations done with the Iwasaki gauge action on the $24^3 \times 64$ lattices of a similar $m_\pi L$, confirming our previous observation of the $m_\pi L$-scaling, which is an indication of finite volume effects. The result from the light ensemble benefits greatly from the application of the AMA method, and its statistical error has gone down from the previous 8% to roughly 3%.
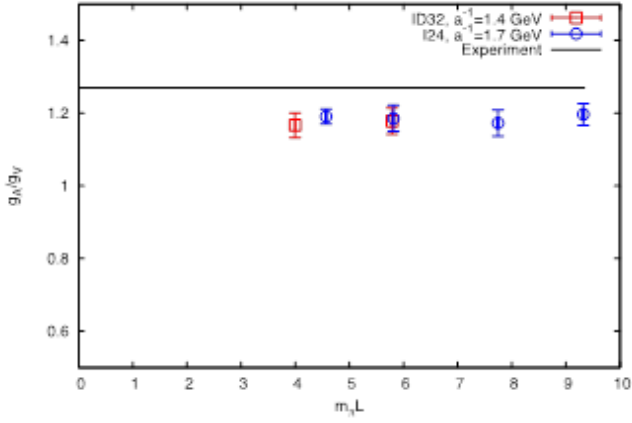
Figure 6: Nucleon axial charge as a function of the product of pion mass and the lattice extent, $m_\pi L$. The red points are the new results from the DSDR+I lattices as calculated on RICC and US NSF TeraGrid/XSEDE resources.

3.2 Nucleon vector form factors

Nucleon vector form factors can be measured experimentally through elastic electron-proton scattering. And the results can be used to determine the proton (p) and neutron (n) charge radii, magnetic moments and the magnetic radii. In our calculations, we have not included the disconnected diagram contribution as shown in Figure 4, which limits us to study only the isovector quantities (difference between proton and neutron). We have now analyzed the data from both the 170 MeV and 250-MeV ensembles, and the preliminary results are shown in Figure 7 and Figure 8, which represent the nucleon isovector Dirac form factors $F_1(q^2)$ and the Pauli form factors $F_2(q^2)$, respectively. In each figure, we show the results for the 170 MeV ensemble from both the full AMA analysis, and the exact calculations to compare. The exact analysis includes about 150 configurations, with 4 sources each. The AMA analysis includes data from around 40 configurations, with 112 sources each, leading to a factor of 2 to 3 reduction in the statistical errors.

We also determined the root-mean-squared (r.m.s.) radii corresponding to the Dirac and Pauli form factors, $\left\langle r_1^2 \right\rangle^{1/2}$ and $\left\langle r_2^2 \right\rangle^{1/2}$ respectively, from dipole fits to the form factors. The results, along with results from earlier calculations at heavier pion masses, are shown in Figures 9 and 10. While chiral extrapolations are needed to connect our results with the experiment, the upward trends shown in Figures 9 and 10 are very encouraging.
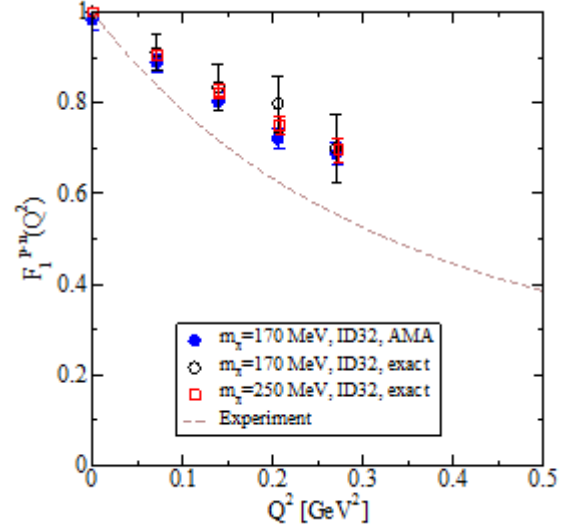


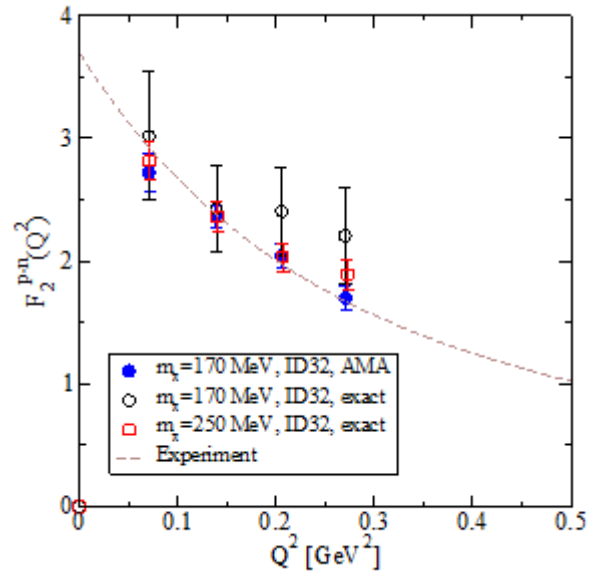Figure 7: Isovector Dirac form factors as a function of the momentum transfer.



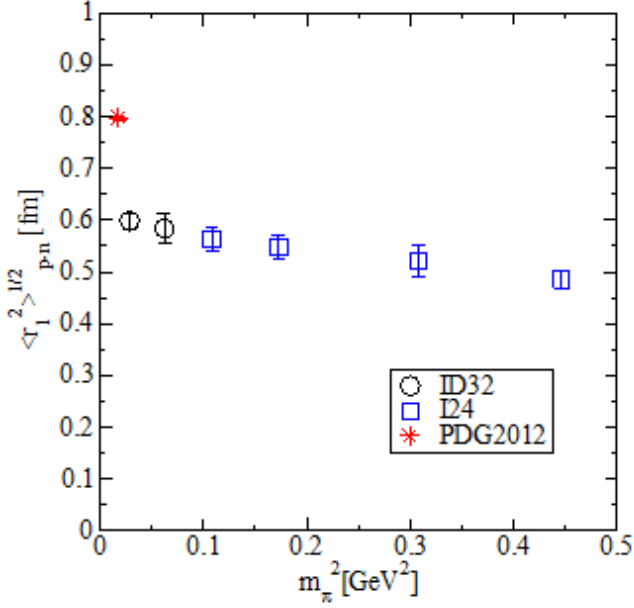Figure 8: Isovector Pauli form factors as a function of the momentum transfer.

Figure 9: The isovector r.m.s Dirac radii. The current results are labeled as "ID32", while results from earlier calculations are labeled as "I24".
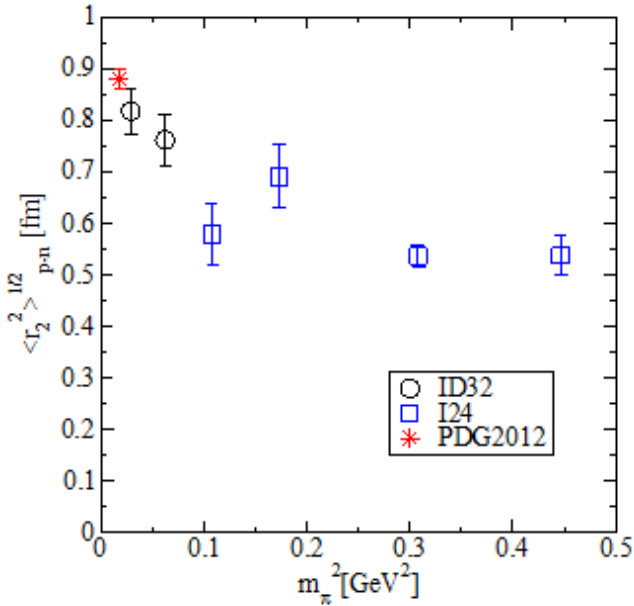


Figure 10: The isovector r.m.s Pauli radii. The current results are labeled as "ID32", while results from earlier calculations are labeled as "I24".

### 3.3 Nucleon mass and strangeness content

As we mention in the Introduction, we can determine the strangeness content of the nucleon by calculating the derivative of the nucleon mass with respect to the strange quark mass. First, in Figure 11 we show our results for the nucleon mass as a function of the pion mass squared. The two blue squares are the results from calculations in our proposal. The rest are from some earlier domain wall fermion calculations. While a chiral extrapolation and a continuum extrapolation are required to compare our results to the experimental value of 939 MeV, our data fall on a smooth curve leading to the physical result, giving us confidence that once our final analysis is done, we will be able to obtain consistent result with the experiment. This serves as a precision test of our techniques and lays convincing ground for our more complex calculations.
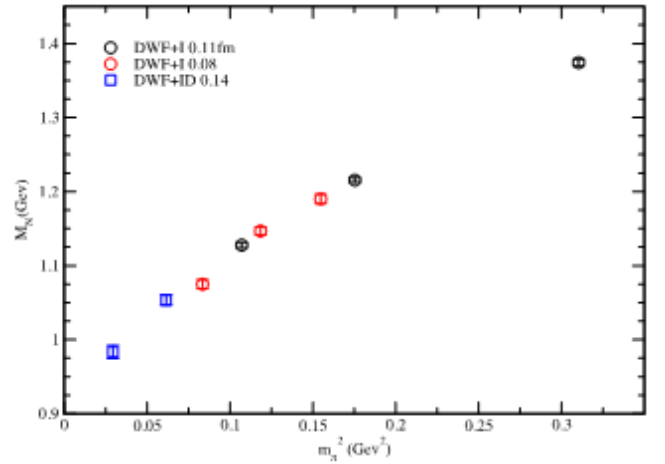


Figure 11: Nucleon mass as a function of the pion mass squared.

While we include only one value for the strange quark mass to generate the gauge configurations, we are able to "reweight" these gauge configurations with a number of different strange quark masses, $m_s$. The results for the nucleon mass with these reweighted strange quark masses are shown in Figure 11. From these results we can extract the slopes of $M_N$ as a function of $m_s$ and determine the strangeness content of nucleon defined as $f_{T_s} = dM_N / dm_s \times m_s / M_N$. In Figure 12 we show the recent results for $f_{T_s}$ from different lattice calculations. The blue squares are from current calculations, which still suffer from large statistical uncertainties and may need more reweighting factors and nucleon correlators to improve the statistical accuracy.
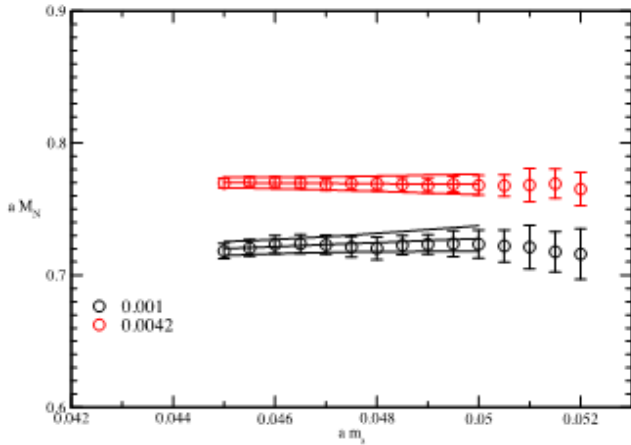
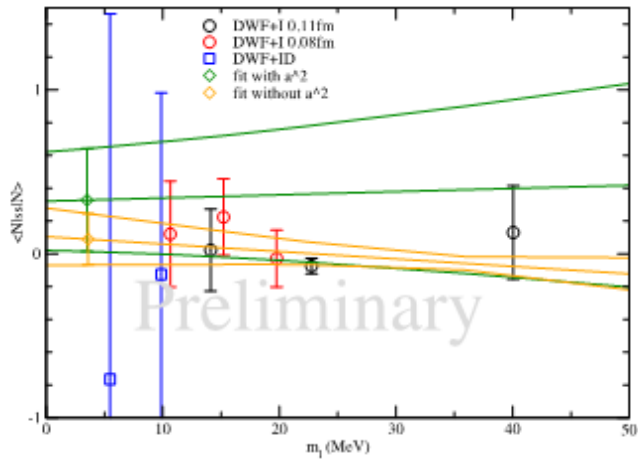Figure 12: Nucleon mass as a function of the reweighted strange quark mass.



Figure 13: Nucleon strangeness content from different calculations.

## 4.    Conclusion

We have made substantial progress towards completing this project. With the application of the All-Mode-Averaging method, it is now plausible to obtain physical results at the light pion masses with 3% statistical error or better with considerably less computing resources than before. This represents a significant advancement in the nucleon structure calculations on the lattice with chiral fermions. These techniques make it possible to achieve high precision calculations with controlled systematic errors.

## 5.   Schedule and prospect for the future

Our calculations in the past three years have allowed us to achieve unprecedented 3% or better error on the nucleon structure observables with chiral fermions at nearly physical pion mass. However, so far we have only done these calculations with a single source-sink separation, a single volume and a single lattice spacing. To have the systematic errors from finite volume and finite lattice spacing under control, we will eventually need to perform calculations in different volumes and at different lattice spacings. Calculations with different volumes and different lattice spacings will require the generation of new gauge configurations, which will be numerically costly and remain a challenge to be tackled in the future.

While we think our source-sink separation is large enough to suppress excited-state contaminations, we would like to perform the calculations at multiple source-sink separations so that a definitive conclusion can be made. With the AMA method, we will now be able to do calculations at a larger source-sink separation with relatively affordable cost. This is what we will propose to use the RICC resources for the next year.

6.   If you wish to extend your account, provide usage situation (how far you have achieved, what calculation you have completed and what is yet to be done) and what you will do specifically in the next usage term.

As we described in Section 2, we have used about 73% of the allocation by March 4, 2013. And by the end of March, we expect to finish 80% of our total allocation if the throughput of our queued jobs remains the same.

The total numbers of exact nucleon three-point functions that have been completed so far are

summarized in Table 2.

Table 2: Nucleon three-point functions completed.

| Pion Mass | # configs. | # sources | Total |
|-----------|-----------|-----------|-------|
| 170 MeV   | 219       | 4         | 876   |
| 250 MeV   | 165       | 8         | 1320  |

These nucleon three-point functions are generated with a source-sink separation of T=9. What we would like to do for the next usage term is to generate nucleon three-point functions at a larger, T=11, separation, with comparable statistical errors. Because the nucleon signal-to-noise decreases exponentially with Euclidean time, achieving the same level of statistical accuracy at a larger source-sink separation inevitably requires more statistics. With AMA, we estimate that 66 configurations, with 256 sources each, will be needed for the 170 MeV ensemble, while 40 configurations with 256 sources each will be needed for the 250 MeV ensemble to achieve a 3% statistical error on gA.

7. If you have a "General User" account and could not complete your allocated computation time, specify the reason.

We project that we will be able to use about 80% of our allocated computation time by the end of the allocation period if we continue to get the same throughput. The reason why we could not use all the allocated time is that we slowed down our running from October to January to implement and test improved computational strategies, specifically, the All-Mode-Averaging method as described in Section 2. Due to the memory limitation of the RICC system, we performed these tests on a cluster in the US while we investigated the best strategies to use on RICC.

References:

[1] C. Allton et al. Phys. Rev. D78:114509, 2008.

[2] J. D. Bratt et al. PoS, LATTICE2008:141, 2008.

[3] J. D. Bratt et al. Phys. Rev. D82:094502, 2011.

[4] H.-W. Lin, T. Blum, S. Ohta, S. Sasaki, and T. Yamazaki. Phys. Rev.D 78:014505, 2008.

[5] S. Ohta. Porceedings of Science, LATTICE 2009:131, 2009.

[6] S. Ohta and T. Yamazaki. LAT 2008:168, 2008.

[7] K. Orginos, T. Blum, and S. Ohta. Phys. Rev. D, 73:094503, 2006.

[8] S. Sasaki, T. Blum, and S. Ohta. Phys. Rev., D65:074503, 2002.

[9] S. Sasaki, K. Orginos, S. Ohta, and T. Blum. Phys. Rev. D, 68:054509, 2003.

[10] S. N. Syritsyn et al. Physical Review D, 81:034507, 2009.

[11] T. Yamazaki, Y. Aoki, T. Blum, H.-W. Lin, M. Lin, S. Ohta, S. Sasaki, R. J. Tweedie, and J. M. Zanotti. Phys. Rev. Lett., 100:171602, 2008.

[12] T. Yamazaki, Y. Aoki, T. Blum, H.-W. Lin, S. Ohta, S. Sasaki, R. J. Tweedie, and J. M. Zanotti. Physical Review D, 79:114505, 2009.

[13] C. Jung. Proceedings of Science LAT2009:002, 2009

[14] T. Blum et al. Phys. Rev., D69:074502, 2004.

[15] S. Ohta for the RBC and UKQCD Collaboration, Proceedings of Science (Lattice 2010), 152 (2010).

[16] S. Ohta for the RBC and UKQCD Collaboration. Proceedings of Tropical QCD (2010).

[17] H. Yin and R. D. Mawhinney. Proceedings of Science LATTICE2011:051, 2011.

[18] M. Lin and S. Ohta. Prog. Part. Nucl. Phys. 67, 218 (2012).

[19] S. Ohta. PoS LATTICE2011 (2011) 168.

[20] Y. Aoki et al. Phys.Rev.D 83:074508, 2011.

[21] R. Arthur et al., arXiv:1208.4412.

[22] T. Blum, T. Izubuchi, and E. Shintani, arXiv:1208.4349

# Fiscal Year 2012 List of Publications Resulting from the Use of RICC

## [Proceedings, etc.]

1. M. Lin and S. Ohta, Finite-size scaling in nucleon axial charge from 2+1-flavor DWF lattice QCD, Proceedings of Science (Lattice2012) 171, 2012.
2. M. Lin, Status of nucleon structure calculations with 2+1 flavors of domain wall fermions, Proceedings of Science (Lattice2012) 172, 2012.
3. C. Jung, Nucleon mass and strange content from (2+1)-flavor Domain Wall Fermion, Proceedings of Science (Lattice2012) 164.

## [Oral presentation at an international symposium]

1. C. Jung, "Nucleon mass and strange content from (2+1)-flavor Domain Wall Fermion", The XXX International Symposium on Lattice Field Theory, Cairns, Australia, June 24-29, 2012.
2. S. Ohta, "Finite-size scaling in nucleon axial charge from 2+1-flavor DWF lattice QCD", The XXX International Symposium on Lattice Field Theory, Cairns, Australia, June 24-29, 2012.
3. M. Lin, "Status of nucleon structure calculations with 2+1 flavors of domain wall fermions", The XXX International Symposium on Lattice Field Theory, Cairns, Australia, June 24-29, 2012.
4. M. Lin, "Nucleon Form Factors and Structure Functions on the Lattice", QCD Structure I workshop, Central China Normal University, Wuhan, China, October 7-20, 2012.

## [Others]

1. S. Ohta, "Nucleon structure from 2+1-flavor dynamical DWF QCD at nearly physical pion mass", RIKEN-Brookhaven Research Center Lunch Seminar, Upton, New York, USA, June 7, 2012.
2. S. Ohta, "Nulceon structure with dynamical 2+1-flavor domain-wall fermions", University of Washington, Seattle, USA, July 10, 2012.
3. S. Ohta, "Finite-size scaling in nucleon axial charge from 2+1-flavor DWF lattice QCD", Kyoto Industrial University, JPS, September 13, 2012.
4. S. Ohta, "Finite-size scaling in nucleon axial charge from 2+1-flavor DWF lattice QCD", JPS, March 26, 2013.